

# Image Processing Tools Applied to Wind Tunnel Testing

Y. Le Sant

Optical Measurement Unit, Department of Fundamental and Experimental Aerodynamics  
Onera, 29 avenue de la Division Leclerc BP 72 Chatillon CEDEX, France  
tel (33) 1 46 23 51 46  
email lesant@onera.fr

## Résumé

Les nouvelles méthodes de mesure optiques telles que la mesure de la pression par Peinture Sensible à la Pression (PSP), la thermographie infrarouge (IRT) et la vélocimétrie par imagerie de particules (PIV) font largement appel à des méthodes de traitement d'image. L'objectif principal est d'ajouter une métrique aux images, en associant à chaque pixel un point réel défini par ses coordonnées 3D. En corollaire, les méthodes surfaciques comme la PSP requièrent l'identification de la position de l'objet dans l'image. Seule l'utilisation de marqueurs placés sur la maquette autorise une reconnaissance d'objet précise. Ces marqueurs sont identifiés et liés à des marqueurs réels. Cela permet ensuite d'identifier le Point de Vue (PDV) de la caméra, qui définit sa position relativement à la scène visualisée. Il est alors possible d'effectuer un alignement d'image précis et d'extraire les informations utiles des images traitées. Les outils de traitement d'image permettent également d'aborder des domaines prometteurs comme la mesure du déplacement et de la déformation des maquettes au cours de l'essai. Enfin, il existe quelques problèmes, comme le traitement de l'auto-illumination, qui nécessitent l'emploi d'outils sophistiqués plus couramment employés en imagerie artificielle.

## Abstract

Image processing tools are needed for new optical measurement methods like Pressure Sensitive Paint (PSP), Infrared Thermography (IRT) and Particle Image Velocimetry (PIV). They are used to transform the pixel coordinates into 3D real coordinates. For surface measurement methods as PSP, the viewed object must be located in the image. The only one way to achieve this requirement is to use markers placed on the model. Their locations in the image is recognized and then they are linked to the real markers. The following action is to identify the Point of View (PoV) of the camera relative to the scene. Then it is possible to make perfect image alignment or to extract accurately information from the image. Image processing tools offer the chance to get more from the images, like the model motion and the model deformation, which are very promising fields of image processing applications. There are also some problems, as the Self-Illumination effect, that use sophisticated image processing tools usually involved in image rendering.

## Introduction

Since a few years, there has been a significant change in wind tunnel instrumentation that is the use of cameras for a wide range of optical measurement methods. Three of them are now well known: Pressure Sensitive Paint (PSP)<sup>1,2,3,4</sup>, Particle Image Velocimetry (PIV)<sup>5</sup> and Infrared Thermography (IRT)<sup>6</sup>. For some recent tests, there is nearly no usual instrumentation as pressure tap and thermocouple. They are replaced by optical methods and only a few of them are installed to check or calibrate the new methods.

This situation is valid for both research wind tunnels and for large wind tunnels, where PSP and IRT are currently applied. The data reduction is more complicated than for sensors and needs more knowledge, especially in image processing. It is not straightforward: many computations are done to convert images in a physical quantity. As a result, optical measurements are done by specialized teams. This leads to a more complex wind tunnel management.

Image processing is a general concept that gathers all the actions that can be done on an image to enhance

one feature or to extract information. A large part of the developed image processing tools is devoted to link the 2D image to the 3D real world. This action is known as image recognition. Let us consider an infrared image in which a model can be seen. This is a quantitative image, however it is really useful only when the model can be found in it, making possible to know the temperature at a given point on the model.

This paper presents what its needed to link the image to the 3D world, as well as miscellaneous possibilities. Optical methods need more actions to convert images into the wanted quantity. These actions are not in the field of image processing since they look like as applying a calibration law. There is one significant exception for the PIV technique because its results depend entirely on image processing tools. However PIV is very well described in many excellent papers<sup>5</sup> and is not in the scope of this paper.

Image recognition concerns many fields as image vision and robotics, where a high accuracy is not needed. This is not the case for image recognition applied to optical measurement methods, which require a pixel or even a sub-pixel accuracy.

Optical methods use cameras and the following section describes how the lens system works and what its main defects are. Then the next section presents two usual ways used to transform 3D coordinates into image coordinates. The markers section addresses how to handle and detect markers placed on the model. A section describes how planar techniques, as PIV<sup>5</sup> and DGV<sup>7</sup> (Doppler Global Velocimetry), can be handled using a simplified approach. For real 3D cases, a 3D linking method (called "resection") is needed and is addressed in details in a specific section. A sophisticated image processing application is briefly presented in the self-illumination section, which is followed by a short conclusion.

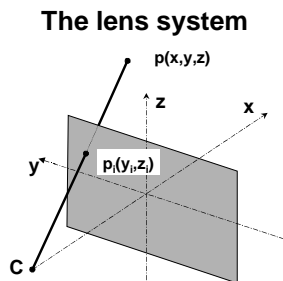


Figure 1: the perspective projection.

The lens system used with the camera provides a planar image of the 3D real scene. It is modeled

using the perspective center assumption, which introduces perspective effects and therefore is known as the perspective projection. The image is formed on the image plane (the CCD) making the intersection with lines coming from the perspective center toward the real object, see Figure 1.

This simple lens model is fully described with only four parameters that are the horizontal field of view  $hF$ , the vertical field of view  $vF$ , the width  $W$  and the height  $H$  expressed in pixels. The image coordinates  $(y_i, z_i)$  related to a point given by its 3D coordinates  $(x, y, z)$  are obtained with the relationship:

$$y_i = \frac{\tan^{-1}\left(\frac{y}{x}\right)}{hF} W \quad z_i = \frac{\tan^{-1}\left(\frac{z}{x}\right)}{vF} H$$

Equation 1: image coordinates.

These equations are very simple and describe a perfect lens system focused at infinity. They can be used without restriction in many cases, but it should be kept in mind that some assumptions<sup>8,9</sup> have been made that are:

- a1 The perspective center C is on the axis of the lens system.
- a2 There is no lens distortion.
- a3 The lens is focused at infinity.

These assumptions can introduce significant errors and must be considered for applications that require a high accuracy level, like PSP. If the related errors cannot be neglected, they must be modeled by using extra parameters called internal camera parameters. These parameters are listed hereafter.

#### a1. Perspective Center

The position of the perspective center is fully described by its coordinates  $(y_c, z_c)$  onto the image plane. This error has nearly no visible effect on the image but it can introduce errors in the assessed position of the camera.

#### a2. Lens distortion

The lens distortion effect is illustrated in Figure 2. It has been numerically enhanced on the left image to make it more visible. It can be compared with the corrected image on the right hand side. The lens distortion is usually described with a polynomial<sup>8</sup>. The number of parameters depends on the importance of the defects. It is not usually greater than four. A typical distortion is the radial distortion, which can be expressed as:

$$dy = K(y - y_c)r^2 \quad dz = K(z - z_c)r^2$$

$$r = \sqrt{(y - y_c)^2 + (z - z_c)^2}$$

Equation 2: lens distortion.

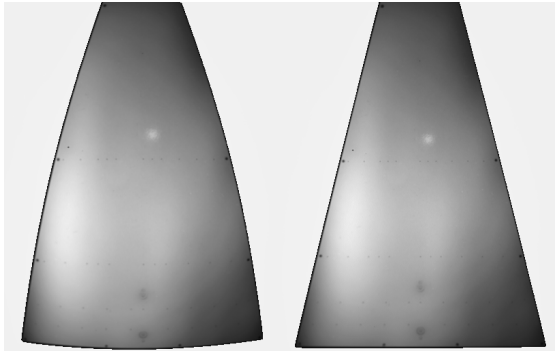


Figure 2: effect of lens distortion.

The usual way to assess the lens distortion effect is to make an image of a calibration card.

### a3. Distance of focus

The perspective model is only valid when the focus is made at an infinite distance. Let us consider in Figure 3 the real case for which the focus is made at a non infinite distance.

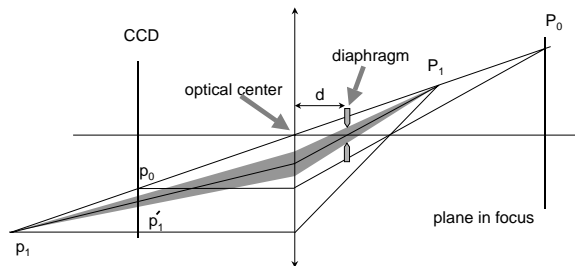


Figure 3: out of focus effect.

A point  $P_0$  is then projected at the point  $p_0$  on the CCD. Now let us consider a point  $P_1$  on the line going from the optical center to the point  $P_0$ . If the focus is made at a long distance,  $P_1$  is also projected on the point  $p_0$ . This is why the perspective center system is used. However the image point  $p_1$  of  $P_1$  is not exactly on the CCD. It forms a spot on the CCD with a diameter depending on the diaphragm aperture. Assuming a small aperture, the spot becomes a single point  $p'_1$ , which can be quite different from  $p_0$ . This effect is called the out of focus effect (OOF).

The only case where OOF disappears is when the diaphragm is exactly at the optical center. Unfortunately this is not the case for usual lens. Figure 4 illustrates this. It shows two images of an emergency system used in wind tunnel. The two images have been taken at the same distance and the aperture was f8, which avoids any significant blurring effect. The focus was made at 1m for the left image and at 1.5m for the right image, where the size of the object is reduced by about 4%.

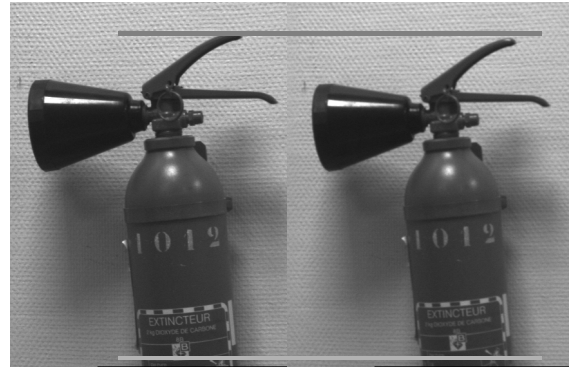


Figure 4: out of focus effect example

Moreover, it can be demonstrated that OOF does not introduce distortion: a straight line becomes a straight line on the CCD. Therefore OOF cannot be suspected, as in Figure 4. It can introduce some conflicts when the object is rather large: no position of the camera can provide the viewed image using the perspective projection.

OOF is different from three others sources of error: it is not a defect of the lens. It can be modeled with only one parameter that is the distance  $d$  between the diaphragm and the optical center. The worse thing is that this distance may depend on the focus distance.

### Assessing internal parameters

The usual way to assess the internal parameters that model the four sources or errors is to make several images of the same target at different locations. The procedure to assess the parameters can be rather complicated. There is a continuous effort to make it more simple and it should be noted that a method<sup>8</sup> using only one image has been recently proposed.

### Camera position and attitude

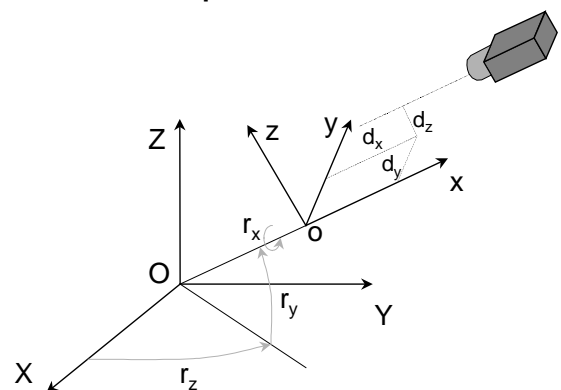


Figure 5: camera position and attitude.

The position and attitude of the camera can be fully described by using three angles and three translations. It is called hereafter Point of View (PoV). A relation can be obtained between the

coordinates in the model system and the coordinates in the camera system. It always can be written as:

$$\begin{bmatrix} x \\ y \\ z \end{bmatrix} = T + R \begin{bmatrix} X \\ Y \\ Z \end{bmatrix}$$

*Equation 3: coordinate transformation.*

where T is a translation vector and R is a 3x3 matrix. Then the lens system transforms the world coordinates expressed in the camera system in screen coordinates using Equation 1.

The problem is how to identify the six parameters describing the position and attitude of the camera<sup>10</sup>. The difficulty comes from the rotation matrix R where the nine coefficients mix cosine and sine of the three angles. This is a non-linear problem and there is no analytical solution.

Developing and using an identification method is not easy. This is the main reason why Equation 3 combined with Equation 1 is often transformed and replaced by the following relationships:

$$y_s = \frac{a_{yx}X + a_{yy}Y + a_{yz}Z + a_y}{b_xX + b_yY + b_zZ + 1}$$

$$z_s = \frac{a_{zx}X + a_{zy}Y + a_{zz}Z + a_z}{b_xX + b_yY + b_zZ + 1}$$

*Equation 4: collinearity equations.*

These equations are widely used in photogrammetry and are known as collinearity equations. They involve eleven parameters. Their big advantage is to enable a direct assessment of the parameters. Given a set of real points (X,Y,Z) and their related positions (y<sub>s</sub>,z<sub>s</sub>) in the image, a linear matrix system can be build and solved using a least square method.

Points used to assess the PoV, either with the matrix system or with the photogrammetry equations, are called markers. Each of them provides two pieces of information. Since the matrix approach handles six parameters (three rotations and three translations), only three markers are needed to identify the PoV. Extra markers are used to overdetermine the system, increasing the accuracy and the reliability of the identified PoV.

On the other hand, collinearity equations require six markers to identify the eleven parameters. As a consequence, the final accuracy of the PoV recognition is lower. But it should be considered that the large number of parameters is used to cope with errors introduced by the internal parameters<sup>8,11</sup>.

An objective comparison of the two solutions is not easy. The collinearity equations are easier to handle and can compensate for defects. Their main disadvantage is that they do not provide the real

angles and translations. If they are required, it is better to use the matrix approach.

## Markers

As it has been previously stated, markers are needed in order to identify the PoV of the camera. Markers are placed (painted marks, holes...) especially for PoV recognition. They can also be visible features of the model as pressure taps.

The contours of the model are not suitable as markers since they are often not clearly distinguishable, even with advanced image processing tools. This comes from blurring effect and from lightning conditions. Anyway, it is always difficult to recognize a contour with an accuracy better than one pixel. This accuracy is not too bad, but it is not sufficient for an accurate PoV recognition.

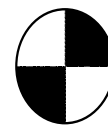


*Figure 6: marker for position and orientation.*

Markers are black or white disks placed on the model. This type of marker allows only to recognize the position, not the orientation. If the orientation is needed, markers as for crash tests must be used, see Figure 6.

The markers should be recognized with a sub-pixel accuracy. This is why they should not be too small: a 1 pixel marker does not enable an accuracy better than 1 pixel. They also should not be too big. One reason is that they do not provide any information for methods like PSP and IRT. The second reason is that the sub-pixel accuracy comes mainly from the border of the marker. The inner part of the marker is useless.

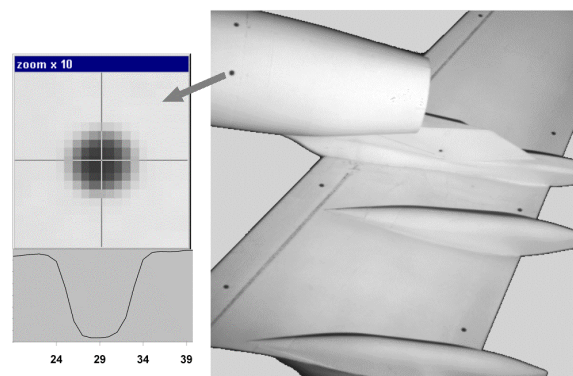


*Figure 7: a too large marker.*

Figure 7 is a PSP application on a commercial aircraft model. It shows a horizontal cut along a too

large marker. Its diameter is roughly 10 pixels and half of this size is not useful.

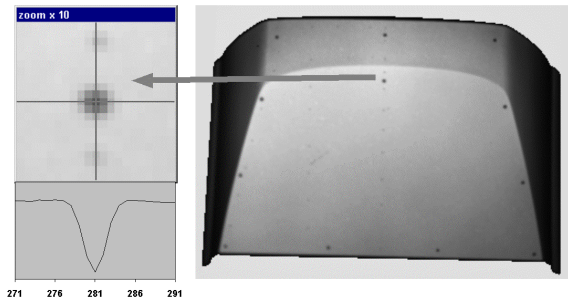


Figure 8: a 5 pixels marker.

Figure 8 is another PSP image made on the rear window of a car. Markers are smaller, since their diameter is 5 pixels. Two gray points can be hardly seen in the zoom window. They are pressure taps drilled in the model. The cut is made along the horizontal axis. It shows that there is no flat area in the marker.

Finding the marker position is done by using correlation functions. The correlation function can be a top hat shape or a cone shape as shown in Figure 9. Both of them are defined by one parameter that is the diameter. The depth of the marker is a result of the identification process.

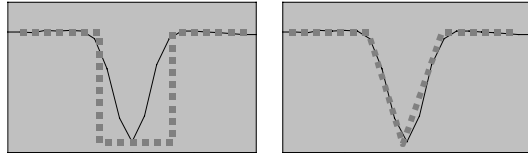


Figure 9 : two correlation functions.

The depth of the marker can be roughly assessed by using a simple image filter as the one presented in Figure 10.

	-1	
-1	4	-1
	-1	

Figure 10: image filter to assess the marker depth.

Real algorithms are more sophisticated and provide a merit value for every pixel. The merit value is a measurement of the agreement with a given shape, as the top hat shape. The lowest it is, the best the local shape looks like to a top hat. Figure 11 is an example of a merit image obtained by using the image in Figure 7.

A threshold is applied on the merit image to eliminate pixels that cannot be markers. An extra operation is needed to obtain a sub-pixel accuracy. The best solution is to adjust the marker position in order to fit as best as possible with the local shape. This solution is rather time consuming so the usual one is to determine the marker position by using a local weighted function.

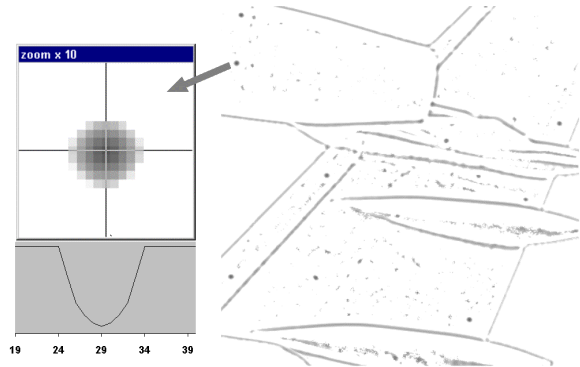


Figure 11: a merit image.

The accuracy of marker recognition depends on many factors, among them the diameter is very important. From our experience, it comes out that the diameter of the markers should not be smaller than 3 pixels and not greater than 10 pixels. The obtained accuracy is then close to 0.1 pixel<sup>11</sup>.

### Planar mapping methods

Typical planar mapping methods are PIV<sup>5</sup> (Particle Image Velocimetry) and DGV<sup>7</sup> (Doppler Global Velocimetry). These methods use a laser sheet, which is viewed with a camera. The measurement system provides a piece of information at every pixel (velocity for both PIV and DGV) and comes the question to identify the position of the camera.

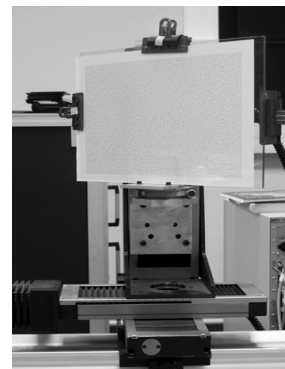


Figure 12: a calibration card used for 3D PIV.

This is done by using a calibration card that can be as simple as a millimeter paper properly set in the scene. Figure 12 is an example of calibration card

used for stereoscopic PIV. The perspective effect is clearly visible on it.

It is then quite easy to recognize some markers on the image and to link them to real 3D locations. Afterwards the eleven parameters of the collinearity equations can be identified. Markers can be recognized manually or with a dedicated tool. Anyway it does not matter because this procedure has to be done only once for the test.

### 3D mapping methods

Mapping techniques as PSP (Pressure Sensitive Paint) and IRT (Infrared Thermography) are addressed in this section. The great differences with planar mapping methods are:

- + the viewed objects are 3D;
- + the objects may move during the test;
- + a lot of images have to be proceeded.

The following go through an IRT example because it will also be used to demonstrate the efficiency of image processing tools to record the model motion during the test. An other reason is that image processing is more difficult to apply on infrared images: for instance, the model contours are scarcely visible because the emissivity factor drops down at high angles. The contrast is often quite low. All of this leads to use markers, as presented in Figure 13.

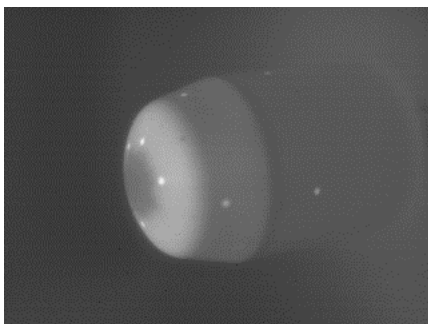


Figure 13: IR image (supersonic test).

The model is the top part of a launcher. Markers are holes drilled and filled with plaster. Plaster is an insulating material, therefore its temperature increases faster than the surrounding material. This makes them visible, but they are difficult to recognize at the beginning of the run. This is why this type of test is a great challenge for image processing tools.

The actions to be performed are:

- + to identify some image markers;
- + to link these image markers to real markers;
- + to identify the PoV of the camera;
- + to extract information from the image.

All these actions are gathered into a single concept named "resection". The IRT example has been proceeded with the Onera's resection software<sup>12</sup>. There are not too many resection softwares around the world, and as far as we know they use the same principles.

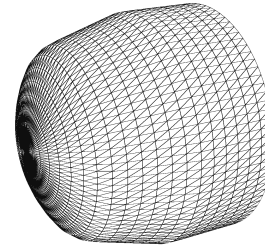


Figure 14: used grid for the IR model.

A grid of the model is required to support the link between the image and the real world. Figure 14 is the grid used for the IRT test.

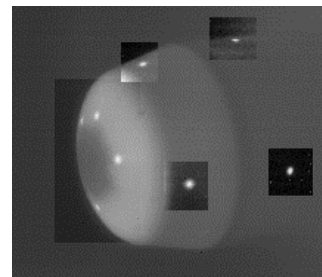


Figure 15: image enhanced.

The image should be enhanced before to recognize the image markers. Enhancement can be made on the whole image or only on limited parts of it. In the present case, the model does not move too much, which enables to predefine areas where the markers should be. These areas are used to enhance the image locally, as in Figure 15, where the markers are clearly visible.

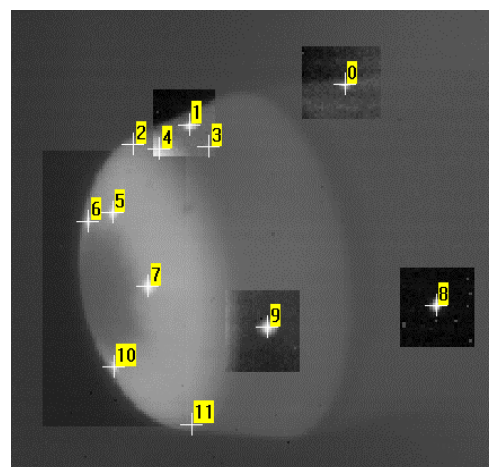


Figure 16: possible candidates.

Then the tools described in the marker section are applied. They enable to find out in the image pixels that could be markers, see Figure 16. All the image markers have been found (0 1 5 6 7 8 9 10), but there are also wrong candidates (2 3 4 11).

The image markers have now to be linked to real markers. This must be done with automated tools called matching tools. However, most of them must be initialized with already linked markers.

Figure 17 shows the linking tool included in the Onera's resection software. The user selects real markers in the list and links them to image markers. Image markers that are only wrong candidates are thrown away automatically.

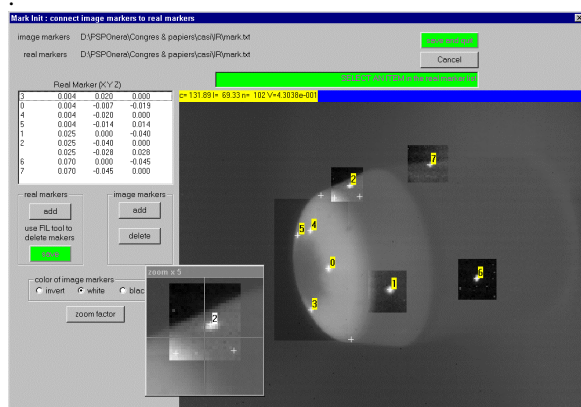


Figure 17: linking candidates to real markers.

Linking manually markers is done only once. For the remainder, image markers detection is followed by a matching step. Figure 18 is an example of an early IR image when the heating process is low. The markers can be hardly seen on the model, and one of them (number 0 in Figure 16) is missing.

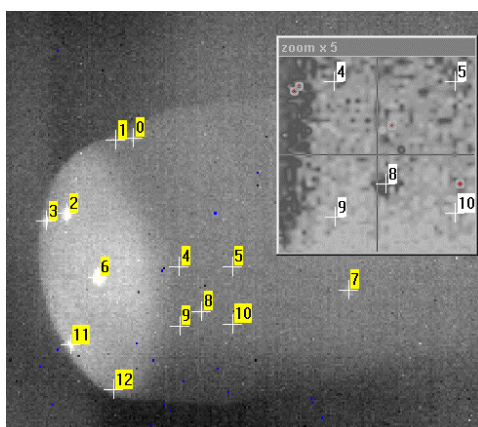


Figure 18: marker detection for an early image.

Matching is a common task in image processing, for instance in machine vision. However the matching

step applied to wind tunnel is different since it must be perfect. Usually there are a many markers in living scene and it does not matter if some of them are mismatched.

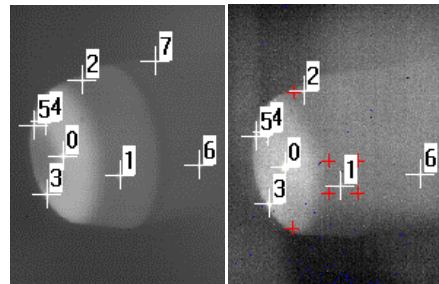


Figure 19: marker matching.

The Onera's matching algorithm is based on statistics. It uses an already matched set of markers. Then three of them are selected and arbitrarily linked to three candidates. These three pairs of markers enable to fit a polynomial function, which is applied to the remainder of the original set of markers (left image in Figure 19). Their new locations in the current image (right image in Figure 19) are compared to the existing candidates. When markers are close enough, they are stated as linked. All the possibilities for the three pairs of markers are checked and the one that provides the highest number of linked markers is the right one.

Once the image markers have been linked, manually or by using a matching tool, it remains to identify the Point Of View (PoV) of the camera. Either collinearity equations or the matrix approach can be used, but the matrix system is more suitable for 3D models. The three rotations and the three translations are identified with an iterative algorithm using a least square method. The computation time is much more lower than the markers recognition time, so there is no disadvantage in using the matrix system.

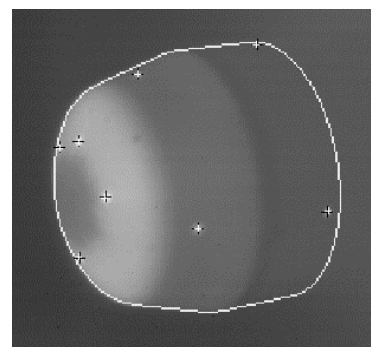


Figure 20: PoV identification.

Figure 20 shows the result of the PoV identification. The grid contour is superimposed on the image. The identified markers are also displayed altogether with

their assessed positions according to the identified PoV. The discrepancy between the two sets of markers is a measurement of the PoV accuracy. In the present case, the accuracy is 0.4 pixel, which is pretty good for IRT. For PSP applications, the accuracy can be better, typically 0.2 pixel. Large errors, more than 2 pixels, mean that something is wrong. Usually the errors come from the real positions of the markers, which can be difficult to measure accurately. A potential source of errors is the model deformation. This question is addressed in the following chapter.

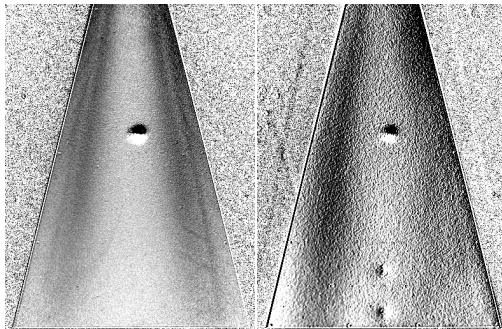


Figure 21: effect off a 1 pixel motion on PSP.

When the PoV has been identified, it is possible to extract information from the image since every pixel is linked to a real point on the model. Another purpose of resection is to align images. This is especially important for PSP applications, since an error of 1 pixel can damage the final pressure image. Figure 21 is an example of PSP application at low speed. The images are obtained by dividing two images. The left one uses perfectly aligned images and the right one shows the noise introduced by a lateral motion of only one pixel.

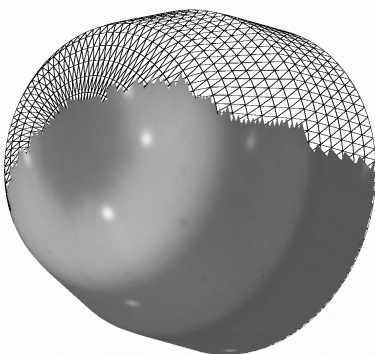


Figure 22: 3D virtual image

Resection enables a perfect image alignment since it provides virtual images according to a given PoV, as the one presented in Figure 22. This type of image can be helpful to get a better understanding of the flow behavior. For instance, the axisymmetric pattern

appears clearly in this virtual 3D view, beside it is not evident in the original image in Figure 13.

### Object motion and object deformation

Resection was needed for the described IRT test because the model moved at the beginning of the test. All the images had to be aligned. The camera image rate was 50 images per second and the duration of the test was 10s. This led to an amount of 500 images to align for each test. This is this huge amount of information that pushed the development of a macro system.

One interesting result is the tracking of the markers along the test. Figure 23 is the record of the marker 0 in Figure 19. The motion is quite large, 8 pixels in the vertical axis and becomes nearly steady after 0.8s, which corresponds to the flow establishment in the test section. Some vibrations are observed after 2s, which are clearly visible in the original infrared film.

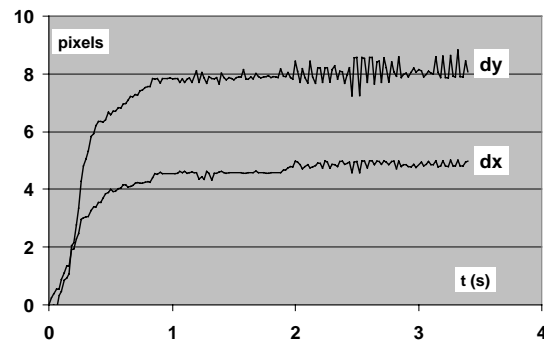


Figure 23: model motion during the test.

It was not planned to use the model motion but it could do. Typically the motion is due to loading, which modifies the model attitude and position. Here comes out an interesting and new possible use of image processing: determination of the real attitude and position of the model.

The most difficult requirement to achieve this goal is to ensure that the camera does not move during the test. This seems quite simple to fulfill, but real applications are rather difficult since everything moves in the test section!

A related field of application is to measure the model deformation. The basic idea is to use the marker positions to assess the model deformation<sup>13</sup>. Typically, if the PoV recognition is perfect without wind but exhibits errors with wind, the only explanation is the model deformation. As for assessing the model position, this new field is in its childhood because there are many possibilities<sup>14,15</sup>.

For instance, it seems fruitful to use together several cameras to find out the model deformation<sup>15</sup>.

### A complex application : Self-illumination

Self Illumination (SI)<sup>16</sup> is a problem related to methods using luminescent paints, like PSP and TSP (Temperature Sensitive Paint). The SI effect is illustrated in Figure 24. The camera is looking at a point A and it collects light coming from it. Any other point B emits light too. It emits light in every direction, as toward A. As a result, A receives light from all the other parts of the model, and may reflect it toward the camera. This leads to an optical pollution: the measured light is the sum of the light really emitted by A and reflected light on A.

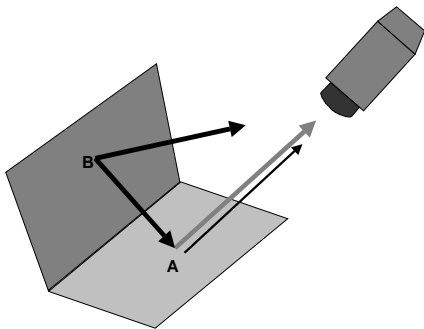


Figure 24: the Self Illumination effect

Figure 25 is a simple example of SI obtained with a corner painted with a PSP. The left image exhibits a significant SI effect near the corner, while this effect disappears in the right image obtained by hiding the left plate of the corner.

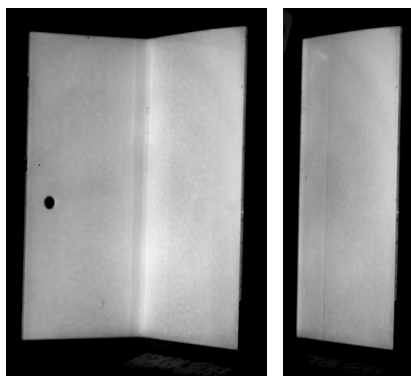


Figure 25: an example of the SI effect

The SI effect falls in the wide field of image rendering, because it uses the same inputs:

- + the emission model of the paint ;
- + the reflection model of the paint;
- + multiple reflections on the model have to be taken into account.

Image rendering deals with all these problems, and the two last ones lead to a number of studies around the world. The reflection model is known as a BRDF model (BRDF = Bidirectional Reflectance Distribution Function) and may be very complex<sup>17</sup>. Managing with multiple reflections requires to handle properly the model surface, and to check all the possible occultations.

SI applied to measurements method adds an extra difficulty: SI correction is an inverse problem. It can be solved quite simply when both the emission model and the BRDF model are lambertian. However real cases are not so simple and the relevant algorithms are expensive (in the sense of computation time). SI correction has been applied to the case presented in Figure 26 using a real model.

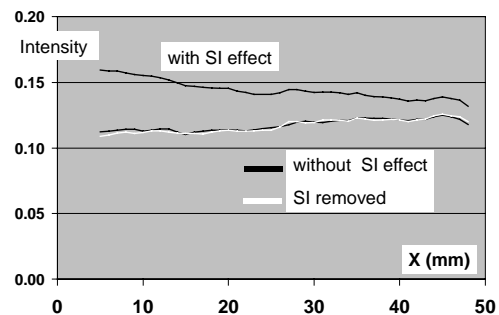


Figure 26: correction of the SI effect

Figure 26 presents the correction of the SI effect along an horizontal line in Figure 25. The SI effect is very large, about 30%, in the corner region. The correction applied is nearly perfect. But real application on PSP tests is still difficult because it takes roughly 5 min to remove the SI effect, while the full resection does not need more than 30s! The remaining problem is then to find out the best compromise between the wanted accuracy and the computation time.

### Conclusion

New optical mapping methods like IRT, PSP, PIV and DGV have led to introduce image processing tools in wind tunnel applications. The common problem of all these methods is to accurately determine the position of the camera. Several softwares have been developed in both research and industrial companies. All of them use markers and sub-pixel algorithms. Although no comparison has been made between these softwares, it is assumed that they provide nearly the same accuracy.

Image processing can now be applied to new promising fields that are model motion and model

deformation. The final accuracy depends on the knowledge of the internal camera parameters and on the camera motion during the test. However, it is expected that both model motion and model deformation will be obtained as a secondary result of methods like PSP.

The SI effect has been briefly described. It demonstrates that even sophisticated image processing tools can be applied in wind tunnel applications. There is no doubt that future optical measurements will involve more and more elaborated image processing tools.

### Acknowledgments

The author wishes to acknowledge Dr Tianshu Liu of NASA Langley and Dr Wim Ruyten of Sverdrup Technology for discussions we had. Discussions with my colleagues Marie-Claire Mérienne, Marianne Lyonnet and Bruno Deléglise are greatly appreciated. Their input pushed the development of efficient tools. Rolf Engler of DLR and Youssef Mébarki of NRC also are acknowledged for their advice and comments that help to develop an user-friendly resection software.

### References

- <sup>1</sup> Sullivan J., "Temperature and Pressure Sensitive Paint", Lecture Series 2000-2001, Advanced Measurement Techniques, Von Karman Institute for Fluid Mechanics, January 2001.
- <sup>2</sup> Bell J.H. and McLachlan B.G., "Image Registration for Luminescent Paint Sensors", 31<sup>st</sup> Aerospace Sciences Meeting & Exhibit, Paper AIAA 93-0178, 1993.
- <sup>3</sup> Troyanovsky I., Sadovskii N., Kuzmin M., Mosharov V., Orlov A., Radchenko V. and Phonov S., "Set of Luminescence Pressure Sensors for Aerospace Research", Sensors and Actuators B, 11 (1993) 201-206.
- <sup>4</sup> Donovan J.F., Morris M.J., Pal A., Benne M.E. and Crites R.C., "Data Analysis Techniques for Pressure- and Temperature-Sensitive Paint", 31<sup>st</sup> Aerospace Sciences Meeting & Exhibit, Paper AIAA 93-0176, 1993.
- <sup>5</sup> Adrian R. J., Durao D.F.G., Durst F., Heitor M.V., Maeda M. and Whitelaw J.H., "Developments in Laser Techniques and Applications to Fluid Mechanics", Springer, 1996.
- <sup>6</sup> Le Sant Y. and Fontaine J., "Application of Infrared Measurements in the Onera's Wind Tunnels", Wind Tunnels and Wind Tunnel Test Techniques, Cambridge, UK, April 1997.
- <sup>7</sup> Samimy M., "A Review of Planar Multiple-Component Velocimetry in High Speed Flows", 20<sup>th</sup> AIAA, Albuquerque, NM, paper 98-2509, June 1998.
- <sup>8</sup> Liu T, Cattafesta L.N. and Radeztsky R.H., "Photogrammetry Applied to Wind-Tunnel Testing", AIAA Journal, Vol.38, Num 6., pp 964-971, 2000.
- <sup>9</sup> Tsai R.Y., "A Versatile Camera Calibration Technique for High-Accuracy 3D Machine Vision Metrology Using Off-the-Shelf TV Cameras and Lenses", IEEE *Transactions on Robotics and Automation*, Vol. RA-3, No.4, pp. 323-344, 1987.
- <sup>10</sup> Penna M.A., "Determining Camera Parameters from the Perspective Projections of a Quadrilateral", Pattern Recognition, Vik.24, No.6, pp. 553-541, 1991.
- <sup>11</sup> Ruyten W., "Toward and Integrated Optical Data System for Wind Tunnel Testing", 39<sup>th</sup> AIAA, Reno, Nevada, paper 99-0581, January 1999.
- <sup>12</sup> Le Sant, Y., Deléglise, B. and Mébarki, Y., "An Automatic Image Alignment Method Applied to Pressure Sensitive Paint Measurements", 17<sup>th</sup> ICIASF, Monterey (U.S.A.), September 29, October 2, 1997.
- <sup>13</sup> Liu T, Barrows A., Burner A.W. and Rhew R.D., "Determining Aerodynamic Loads Based on Optical Deformation Measurements", 39<sup>th</sup> AIAA, Reno, Nevada, paper 2001-0560, January 2001.
- <sup>14</sup> Liu T, Radeztsky R.H, Garg G. and Cattafesta L.N., "A Videogrammetric Model Deformation System and its integration with Pressure Paint", 37<sup>th</sup> AIAA, Reno, Nevada, paper 99-0568, January 1999.
- <sup>15</sup> Ruyten W., "Model Attitude Measurement with and Eight-Camera Pressure-Sensitive Paint System", 38<sup>th</sup> AIAA, Reno, Nevada, paper AIAA 2000-0833, January 2000.
- <sup>16</sup> Ruyten W. and Fichser, C.-J., "On the Effects of Reflected Light in Luminescent Paint Measurements", 38<sup>th</sup> AIAA, Reno, Nevada, paper AIAA 2000-0833, January 2000.
- <sup>17</sup> Lafortune, E and Willems, Y., "Using the Modified Phong Reflectance Model for Physically Based Rendering", Report CW 197, Department of Computing Science, K.U. Leuven, November 1994.